IMPEDANCE SYNTHESIS FOR HYBRID ANALOG-DIGITAL AUDIO EFFECTS

Francisco Bernardo
Dyson School of Design Engineering
Imperial College London
London, UK
f.bernardo@imperial.ac.uk

Matthew Davison
Dyson School of Design Engineering
Imperial College London
London, UK
m.davison23@imperial.ac.uk

Andrew McPherson
Dyson School of Design Engineering
Imperial College London
London, UK
andrew.mcpherson@imperial.ac.uk

ABSTRACT

Most real systems, from acoustics to analog electronics, are characterised by bidirectional coupling amongst elements rather than neat, unidirectional signal flows between self-contained modules. Integrating digital processing into physical domains becomes a significant engineering challenge when the application requires bidirectional coupling across the physical-digital boundary rather than separate, well-defined inputs and outputs. We introduce an approach to hybrid analog-digital audio processing using synthetic impedance: digitally simulated circuit elements integrated into an otherwise analog circuit. This approach combines the physicality and classic character of analog audio circuits alongside the precision and flexibility of digital signal processing (DSP). Our impedance synthesis system consists of a voltage-controlled current source and a microcontroller-based DSP system. We demonstrate our technique through modifying an iconic guitar distortion pedal, the Boss DS-1, showing the ability of the synthetic impedance to both replicate and extend the behaviour of the pedal's diode clipping stage. We discuss the behaviour of the synthetic impedance in isolated laboratory conditions and in the DS-1 pedal, highlighting the technical and creative potential of the technique as well as its practical limitations and future extensions.

1. INTRODUCTION

Virtual analog modelling, or the digital simulation of nonlinear analog circuits, remains a topic of considerable interest in audio research [1, 2]. Virtual analog circuits offer practical advantages over their physical counterparts, including cost, precision, flexibility and replicability. By necessity, however, many elements of audio systems must remain analog, including pickups, microphones, loudspeakers (and their associated amplifiers), acoustic instruments and of course the human body itself. The question for audio system designers thus turns to where to draw the boundaries between physical and digital domains. In audio, boundaries are typically drawn through directed signal flows between self-contained units: signals flow from (low-impedance) outputs to (high-impedance) inputs and not vice-versa. Where digital audio processing is incorporated into analog systems, digital and analog regions are typically separated by such an impedance boundary which allows well-defined inputs and outputs from each region. Alternatively, digital systems can manipulate the parameters of an analog circuit through control voltages (CVs) or digital potentiometers, which are also typically unidirectional in their effect.

More challenging is true bidirectionality, where audio-rate signals flow flexibly back and forth between digital and analog domains across a single junction. Bidirectional coupling and mutual influence amongst components are intrinsic properties to most physical systems, including acoustic instruments and analog electronics [3]. Integrating bidirectionality into different layers of audio technology holds promise for tighter physical-digital integration with particular applications in musical performance, including more intimate control of sound synthesis [4] with interfaces supporting collocated sensing and actuation [5]. Implementing this bidirectionality with digital systems remains a conceptual and practical engineering challenge [6].

This paper proposes an approach to creating hybrid digital-analog audio circuits where the relationship between domains is intrinsically bidirectional. Drawing on research from active vibration control [7], we implement a digitally simulated analog circuit element whose impedance is programmable using real-time digital signal processing. One or more such elements can be incorporated into an analog circuit, including classic guitar pedals or synthesisers, as a replacement for obsolete or unreliable components or as a form of creative modification or circuit bending [8].

The contributions of this paper include a technique for simulating analog circuit elements with digital impedance modelling and a practical implementation of the synthetic impedance system using an embedded digital signal processing (DSP) board. We demonstrate an application of the synthetic impedance by replacing and subsequently modifying the diode clipping stage in the classic Boss DS-1 guitar distortion pedal. Results show that the synthetic diodes have similar behaviour in the actual pedal as the original diodes they replace, while being easily reprogrammable in software. Section 2 of the paper lays the theoretical foundations, while Section 3 details the circuits and signal processing of our implementation. Section 4 presents a case study with the DS-1, whose results are summarised in Section 5. Section 6 discussions the implications, limitations and possible extensions of this work.

2. BACKGROUND

2.1. Modularity and Unidirectionality in Audio Systems

Modularity is a foundational principle of engineering. The design and analysis of complex systems is greatly simplified when they can be separated into discrete, self-contained subcomponents with intrinsic properties that are insensitive to what they are connected to. Components of audio systems, including synth modules and effects units, typically exhibit an *impedance bridging* property [9] where connections are made from the low-impedance output of one unit to the high-impedance input of the next. In the idealised case of zero output impedance and infinite input impedance, the

operation of each unit is entirely independent of what it is connected to, with no crosstalk or loading effects (at least in cases without feedback loops). Digital audio systems typically also adopt this rigid distinction between inputs and outputs, reinforced by the unidirectional behaviour of analog-to-digital and digital-to-analog converters (ADCs and DACs) and even the design of microprocessors themselves, where distinctions between data inputs and outputs are encoded at an electrical register level [6].

The unidirectional signal flow model is a convenience, not a necessity [6]. In RF engineering (amongst other domains), impedance matching (rather than bridging) is commonplace to promote maximum power transfer and minimise signal reflections. In acoustic systems including musical instruments, vibrating structures mutually influence one another, and the behaviour of the whole system can only be understood by analysing the interdependencies of components. For example, in reed instruments, tone production depends on mutual coupling between lip force, reed stiffness and reflected waves in the air column of the instrument [10], while on the guitar, the mutual coupling of strings and body affects both the projected acoustic sound and the decay time of the strings themselves, often in frequency-dependent ways [11].

At a basic electrical level, all circuits involve mutual dependencies between individual components rather than directed signal flows; the entire history of virtual analog modelling has grappled with how to efficiently deal with these (often nonlinear) relationships in a computationally tractable way [12]. In many practical cases, these mutual dependencies extend across boundaries of nominally independent devices. For example, electric guitar pickups exhibit frequency-dependent impedance of tens or hundreds of kilohms across the audio range [13], which interacts with the finite input impedance of most amplifiers. Confounding the input/output distinction has been the locus of many experimental practices, including feedback musicianship [14, 15] and the synthesisers of Peter Blasser, which introduce "sandrodes" or "androgynous" circuit nodes functioning as both inputs and outputs and defying traditional unidirectional signal flows [16].

2.2. Analog Modelling and its Limitations

A classical method of analysing electronic circuits involves *nodal analysis* in the Kirchoff domain: a system of ordinary differential equations (ODEs) can be written involving the voltage at each node of the circuit, the currents through each component, and the (possibly nonlinear) impedances of each circuit element. Solving this system of ODEs becomes computationally expensive for large circuits, and the presence of nonlinearities often requires the use of iterative algorithms such as Newton-Raphson. In audio, even a relatively simple a diode clipper circuit with an embedded low-pass filter – the foundation of distortion pedals – requires an iterative approximation approach to solve a nonlinear ODE [17].

Wave Digital Filters (WDFs) [18] have proven enduringly popular for virtual analog modelling, including of nonlinearities [19]; WDFs reformulate the familiar Kirchoff variables into incident and reflected wave variables. Classical WDFs allowed a single nonlinearity to be simulated at the root of the WDF tree, though more recent work has enabled the simulation of circuits with multiple nonlinearities [20, 21]. Recent research on WDFs also focused on more efficient and/or non-iterative methods [1, 2], including solving the diode nonlinearity analytically with the Lambert W function [22], or through its approximation using the Wright Omega function [23].

Aside from these ongoing computational challenges, our work is motivated by a conceptual conundrum in virtual analog (VA) modelling: *where does the simulation end?* If a VA system is used for performance rather than purely for analysis, then there must exist some boundary between the simulation and the analog or digital signals connected to it. Pursuing an accurate and comprehensive model of a complex analog system will push the designer to include more and more of that system in the simulated domain. The natural stopping points are impedance boundaries: low-impedance voltage sources or connections to high-impedance inputs, which might be found within an analog device (for example, at the output of an op amp) as well as at its exterior connections.

However, what if we want to digitally simulate only *part* of an analog circuit, and there are no impedance boundaries separating the part we want to simulate versus the part we want to leave in its original form? What happens if the connection to the audio source does not lend itself to the idealised impedance bridging situation to begin with (e.g. for certain guitar or microphone preamplifiers)? Does the simulation then need to extend to the instrument and even the player? There is an opportunity for digital simulation which can co-exist flexibly with literal analog systems.

2.3. Synthetic Impedance

One approach to integrating digital and analog systems is to create a digital facsimile of an analog component, which can then be integrated into a circuit similarly to the original. This idea is commonly known as *synthetic impedance* (or admittance [7]), and it can be found in many domains including acoustics [24] and meta-materials [25]. In electronics, a synthetic impedance involves a voltage-controlled current source (VCCS) designed to emulate an arbitrary two-terminal circuit element by establishing an arbitrary relationship between input voltage and output current. Research on driving-point impedance as a function of frequency dates back to the early 20th century, with Foster's Reactance theorem [26], and Brune's synthesis of arbitrary two-terminal networks with frequency-dependent impedance [27].

More recently, digital impedance synthesis has been gaining traction in instrumentation engineering, material science and vibration control. This approach uses a DSP unit alongside a current source to simulate circuit components, which can be linear or nonlinear, as well as static or time-varying. Fluke Corporation patented a programmable impedance synthesiser circuit to support calibration processes that previously relied on discrete, well-characterised reference components [28]. Fleming et al. [7] introduced a synthetic impedance circuit for piezoelectric shunt damping in electro-acoustic absorbers. Their approach was based on the principle that precise tuning of the electrical resonance frequency of electro-acoustic absorbers to match that of the host structure can effectively mitigate structural vibrations.

Subsequent research expanded on Fleming's approach by shifting signal processing to standalone embedded devices. Plíva et al. implemented digital impedance synthesis using an FPGA [29], which had limited sampling resolution and accuracy. Matten et al. [30] further enhanced digital synthetic impedance by improving circuit precision and algorithms for piezoelectric shunting, with experimental validation. Necásek et al. [31] used an ARM Cortex-M4F microcontroller with 18-bit Successive Approximation Register (SAR) converters to enhance resolution and minimise pipeline delay. More recent work began to explore nonlinear impedance synthesis [32, 33].

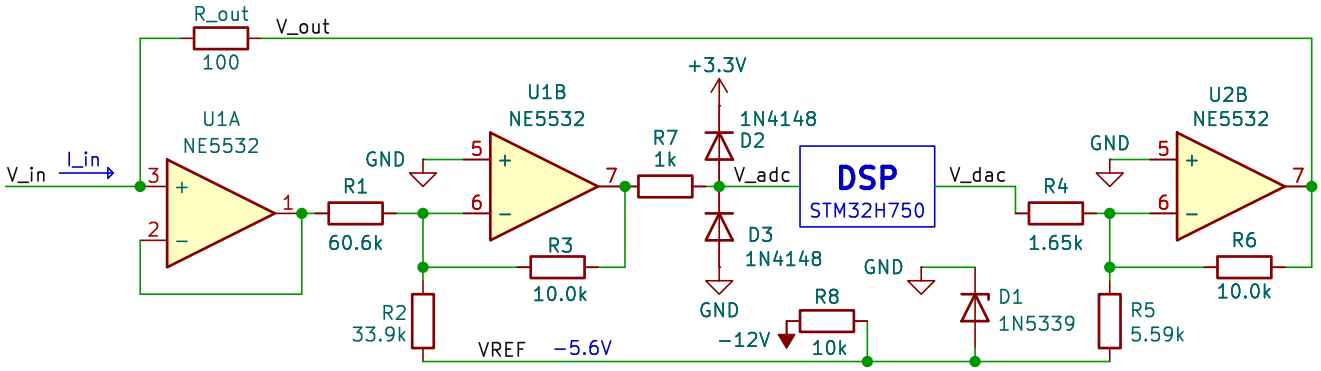

Figure 1: *Synthetic impedance schematic, implemented as a voltage-controlled current source. Digital signal processing, ADC and DAC use a STM32H750 microcontroller; op amps powered from ±12V provide buffering and level shifting to cover a ±10V range of input signals. Precision in component values is important to achieving good performance.*

3. SYNTHETIC IMPEDANCE IMPLEMENTATION

We implement a two-terminal simulated analog circuit element which takes the form of a programmable voltage-controlled current source (VCCS; Section 2.3). By changing the relationship between voltage and current, different circuit elements can be simulated including arbitrary combinations of resistors, capacitors and inductors, as well as nonlinear elements such as diodes.

3.1. Hardware

Figure 1 shows a schematic of the synthetic impedance element, derived from a classic analog gyrator topology. The centre of the circuit is a real-time digital signal processor based on an STM32H750 microcontroller, which includes an ARM Cortex-M7 processor, a 16-bit SAR ADC and a 12-bit DAC.

The behaviour of this circuit as a controllable current source depends on the output voltage V_{out} and resistor $\mathrm{R_{out}}$:

$$I_{in} = \frac{V_{in} - V_{out}}{\mathrm{R_{out}}} \tag{1}$$

The effective input voltage range for the synthetic impedance element is ±10V. The unity gain buffer U1A ensures I_{in} depends only on V_{out} with no other input current. The summing amplifier U1B implements a level shifter to map this input voltage range to the 0-3.3V range of the ADC. Resistor R7 and diodes D2-D3 provide input voltage protection for the ADC. The summing amplifier U2B implements a level shifter to map from the DAC's output range of 0-3.3V back to the full range of ±10V.

For best performance, the two level shifters must be precisely calibrated in gain and offset so that together they exhibit unity gain and zero offset voltage from input to output, and so that 0V at the input of the synthetic impedance corresponds exactly to the midpoint of the ADC range. Note that since U1B and U2B are inverting amplifiers, the voltages seen by the DSP are inverted compared to the input terminal of the circuit element.

Our implementation assumes that one of the two terminals of the synthetic impedance is connected to ground, though the circuit could be extended with a differential input stage and a second output to allow for simulation of floating impedance elements.

3.2. Signal Processing

The firmware of the STM32H750 implements an unbuffered (single-sample) real-time DSP system operating at a sample rate of 70kHz. Samples are processed in floating point, with volts as units (i.e. taking a range of -10 to 10).

The DSP system implements an admittance function $Y(s) = I(s)/V(s)$, which for linear circuit elements can be implemented using IIR filters transformed from continuous to discrete time using a bilinear transform with pre-warping. Given a discrete-time current $i_{in}[n]$ corresponding to Equation 1, the signal to the DAC (in volts) is calculated as:

$$v_{DAC}[n] = v_{ADC}[n] - \mathrm{R_{out}} i[n] \tag{2}$$

The signal $\mathrm{v_{DAC}[n]}$ is then renormalised from a ±10V range to the full output range of the DAC (0-4095 for a 12-bit DAC).

3.3. Calibration and Performance

With the built-in ADC and DAC on the STM32H750 and a 70kHz sample rate, the system exhibits an end-to-end latency of 11μs (including settling time of the ADC and DAC). Since latency corresponds to a linear phase shift with respect to frequency and $\mathrm{R_{out}}$ provides a feedback path from output back to input, this digital processing latency places constraints on the usable bandwidth if the system is to remain stable.

There are two approaches to bandwidth limiting for stability. A capacitor can be placed across the terminals of the synthetic impedance, attenuating the gain V_{in}/V_{out} at high frequencies. Additionally, a first-order IIR low-pass filter can be incorporated into the DSP routine with a cutoff above the frequency range of interest for the input signal. This will contribute its own phase lag of 45° at the cutoff frequency, so its cutoff should be chosen carefully.

4. CASE STUDY

4.1. Boss DS-1 Distortion Pedal

The Boss DS-1[1], made by Roland and first introduced in 1978, is a classic distortion pedal known for its signature hard-clipping

[1]BOSS DS-1 Distortion, `https://www.boss.info/global/products/ds-1/`, accessed: 2025-06-13

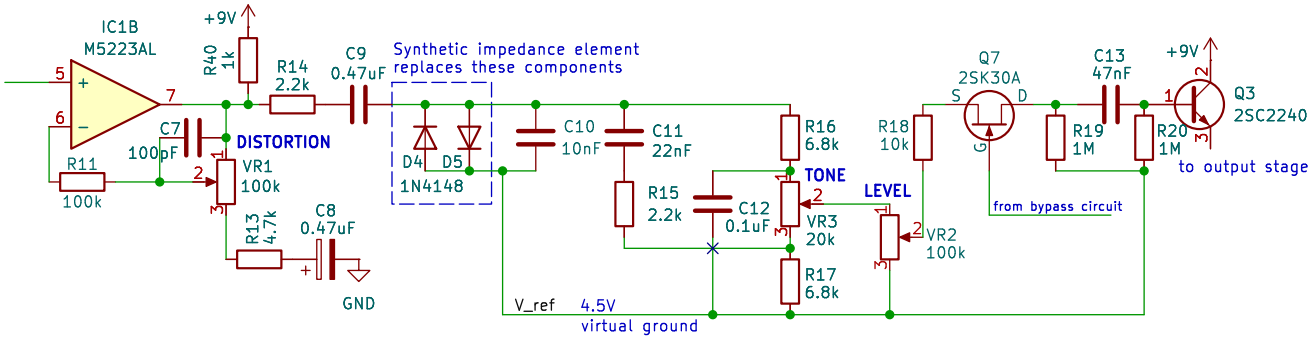

Figure 2: *Clipping and tone stages of the Boss DS-1 (2006 version), based on [34]. Diode pair D4/D5 is replaced with a synthetic impedance element in our experiments.*

sound. As Boss's first distortion pedal, it delivers a sharp, high-gain tone commonly used across several decades of rock and metal music. The DS-1 has been previously studied as a reference circuit in non-linear distortion modelling [17].

Over its lifespan, the Boss DS-1 has evolved through several revisions which have been reverse engineered and extensively documented by hobbyists [34]. Each revision has distinct sonic characteristics, but all of them contain a central hard clipping stage with two anti-parallel silicon diodes driven by an op amp (Figure 2), discussed further in the next section. The DIY electronics community has developed a number of popular modifications to the DS-1 circuit, including reconfigurations of the diode clipping stage such as those by Brett Miller and Robert Keeley [34].

4.2. Clipping Stage Analysis

Our case study focuses on the 2006 version of the DS-1 circuit (documented in [34]). The clipping stage and tone control is shown in Figure 2. Since gain stage IC1B provides a low-impedance output, any other components connected to its inputs or outputs will have minimal effect on the clipping stage. Similarly, emitter follower Q3 provides reasonable isolation between the clipping stage and the subsequent components at the output stage of the pedal.

Within the clipping stage and tone control, there is considerable interdependence between components. Silicon diodes D4-D5 (1N4148) provide the main source of nonlinear distortion by shunting the signal to an AC ground point (4.5V). Their clipping behaviour depends on series resistor R14 and low-pass filtering capacitor C10. The mutual dependencies of these four components have been previously analysed by Yeh et al. [35]. The behaviour of this portion of the circuit will also be influenced by any series resistance or non-idealities in DC blocking electrolytic capacitor C9, the RC network in the tone and level controls and any current limiting or other non-idealities of op-amp IC1B. If any components in this stage of the circuit exhibit nonlinear behaviour, then a fully digital simulation of this circuit requires solving for multiple nonlinearities, a notoriously challenging task [21].

Leaving aside the interdependence between components, anti-parallel diodes D4 and D5 can be modelled in the Kirchoff domain using the Shockley ideal diode model:

$$I = I_S(e^{\frac{V_D}{nV_T}} - 1) - I_S(e^{-\frac{V_D}{nV_T}} - 1) \tag{3}$$

where I is the total current through the pair of diodes and V_D is the voltage across them. I_S is the reverse-bias saturation current, V_T is the thermal voltage, and n is the ideality factor or the material constant [36]. Following [22], these values are parametrised for 1N4148 diodes at 300°K with I_S = 2.52 nA, n = 1.752, and V_T = 25.86 mV.

4.3. Introducing Synthetic Impedance into the Clipping Stage

In our case study, we implement Equation 3 in our DSP system from Section 3. The synthetic impedance element is then attached in place of diode pair D4-D5. Since the diodes connect to a virtual ground point of 4.5V and only AC signals are of interest, we use a 470μF capacitor in series with the synthetic impedance, and in the digital domain we include a 1st order high-pass filter at 5Hz prior to the calculation of the nonlinearity (Equation 3) to remove any residual DC offset.

Following Section 3.3, to address stability constraints associated with system latency, the DSP code also includes a first-order low-pass filter at 7kHz prior to the nonlinearity; this is mostly above the frequency range of interest for guitar players, though it will affect on the tone of heavily distorted guitar signals.

5. EVALUATION

The measurements in this section relate to the synthetic anti-parallel diodes described in Equation 3 and Section 4.3. We compare their behaviour with real 1N4148 diodes, measuring both in isolation (out-of-circuit) and within the actual DS-1 pedal. We explore variations in input frequency, amplitude, and pedal control settings.

5.1. Experimental setup and data collection

We use an Analog Discovery 3 [2] for waveform generation and data acquisition. Data was processed with Jupyter notebooks and MATLAB[3] enabling aggregation, conditioning, and visualisation of waveforms and spectra, along with signal analysis. Data is organised into datasets, each corresponding to a unique test configuration including:

[2]Digilent Analog Discovery 3, `https://digilent.com/reference/test-and-measurement/analog-discovery-3/start`, accessed: 2025-06-13

[3]MathWorks MATLAB Online, `https://matlab.mathworks.com/`, accessed: 2025-06-13

- Diode Clipper Type: *Real* anti-parallel silicon 1N4148 pair or *Synthetic* – with configurations 1F1R (one forward, one reverse, matching the DS-1), 2F1R, 4F1R, corresponding to whether the forward D5 diode is replaced with two diodes, or with Brett Miller's "HUEVOS GRANDES" DS-1 mod, with two pairs of parallel forward diodes [34]
- Circuit Context: *in circuit* (DS-1 pedal, with Tone control ranging from 0.0 and 1.0) or *out of circuit* (in isolation, on a breadboard, using only a 2.2kΩ series resistor and 10nF parallel capacitor following Figure 2)
- Input Voltage Levels: ±1V, ±2V (tests were also conducted at ±200mV and ±5V but omitted for brevity)
- Input Frequency: 100Hz, 1kHz (sine waves)

Datasets, processing scripts, plots, tables, and audio are publicly available in: `https://github.com/frantic0/dafx25`

5.2. Time domain analysis

We compare time-domain waveforms clipped by either a real 1N4148 diode pair or a synthetic diode pair, measured both in isolation (out-of-circuit) and within the DS-1 pedal. Figure 3 shows the experimental time-domain waveforms recorded in isolation, out of circuit, at two input frequencies—100Hz and 1kHz—with input amplitudes of ±1V and ±2V. At the given input voltages, all waveforms show that the signal was subject to soft clipping. At lower frequencies, the real and synthetic diode waveforms show a close resemblance. At higher frequencies, however, there are noticeable wave shape inaccuracies, suggesting frequency-dependent deviations discussed further in Section 6.

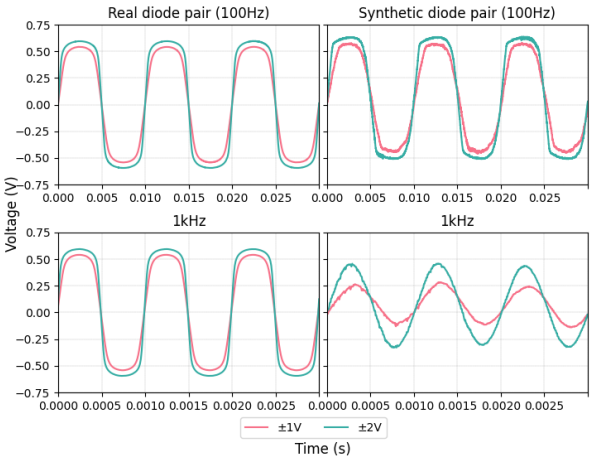

Figure 3: *Experimental results for two diode pairs: real 1N4148 (left) and synthetic (right), measured in isolation (out-of-circuit). Waveforms are shown for input frequencies of 100Hz (top) and 1kHz (bottom) with input amplitudes of ±1V and ±2V.*

Figure 4 presents a comparison of real and synthetic diode clippers within the Boss DS-1 pedal circuit. The experimental results display a 100Hz waveform with input amplitudes of ±1V and ±2V, processed through the pedal. The influence of tone shaping on the clipped waveforms is clearly visible, highlighting the presence of additional nonlinearities in the circuit beyond simple diode clipping. In both in-circuit and out-of-circuit conditions, results indicate that the synthetic diode model effectively replicates the behavior of real diodes, with notable deviations occurring at higher frequencies.

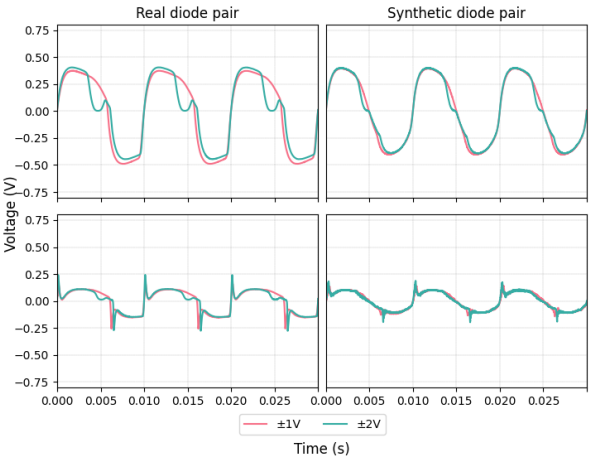

Figure 4: *Experimental results showing a 100 Hz waveform clipped by the real 1N4148 diode clipper (left) or a synthetic diode pair (right), operating within the Boss DS-1 pedal circuit. The waveform has input amplitudes of ±1V and ±2V. Pedal controls for Tone, Level, and Distortion are set to (0.0, 1.0, 0.0) at the top and (1.0, 1.0, 0.0) at the bottom.*

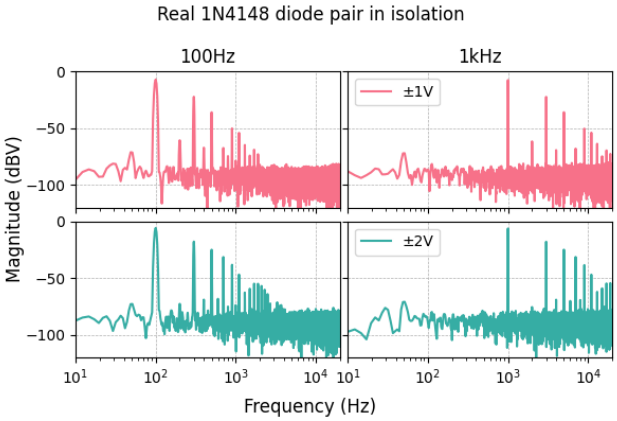

Figure 5: *Spectral analysis of a real 1N4148 diode pair measured in isolation, out of circuit, with two waveforms of 100Hz and 1kHz, with input amplitudes of ±1V and ±2V.*

5.3. Frequency domain analysis

We compare the frequency-domain spectra of signals processed through a real 1N4148 diode pair and a synthetic diode pair, both measured in isolation (out-of-circuit). Figures 5 and 6 present the spectral analysis for the real and synthetic diode pairs, respectively. Both sets of spectral data were obtained using waveforms at 100Hz and 1kHz, with input amplitudes of ±1V and ±2V.

The results show that the synthetic diode model approximates the clipping behaviour of real diodes in the frequency domain. However, notable differences include a generally higher noise floor, especially in the low-end frequencies, and an overall increase in total harmonic distortion (THD).

In Table 1, the test cases are displayed with the measured Total Harmonic Distortion (THD), Signal to Noise Ratio (SNR), and level of the first five harmonics relative to the level of the fundamental. The THD is calculated using the level of the first 10 harmonics; the SNR is calculated by suppressing the first 10 harmonics (including the fundamental). The harmonic levels show that both the real and synthetic pairs produce symmetric clipping with prominent odd harmonics. This can be seen in the 100Hz, ±1V out of circuit measurements in the first two rows of Table 1 for instance. For both the real and synthetic diode pairs, the 3rd harmonic level is over 20dB higher than the 2nd or 4th harmonics. This shows that the synthetic diodes are performing as expected, with symmetric clipping of the waveform.

In contrast, harmonic levels of alternative synthesised diode configurations can be seen in the lower section of Table 1. In these cases, the clipping is asymmetrical due to the difference in diodes. This causes the negative section of the waveform to begin clipping at a different voltage level compared to the positive section. The asymmetrical clipping increases the level of even harmonics compared to the standard diode pair configuration. This can be seen in the *100Hz, ±1V, Tone Control minimum, 2F1R* diode configuration measurement. In this data, the second harmonic is 10.5dB higher than the third harmonic. In the equivalent measurement for the *1F1R Synthetic* configuration, the second harmonic is 2.1dB higher than the third harmonic.

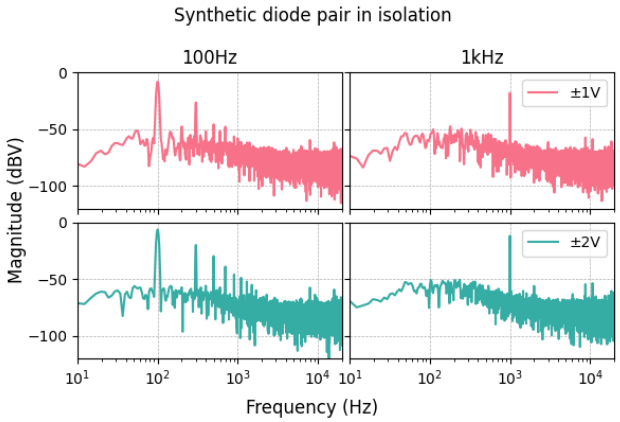

Figure 6: *Spectral analysis of a synthetic diode pair measured in isolation, out of circuit, with two waveforms of 100Hz and 1kHz, with input amplitudes of ±1V and ±2V.*

6. DISCUSSION

The synthetic diodes behave similarly in both time and frequency domain to the real 1N4148 pair for 100Hz stimuli. The DS-1 exhibits complex waveshaping properties at high signal amplitudes (Figure 4), not explainable by diode clipping alone. That the synthetic diodes successfully replicate this combined behaviour shows the potential of this method: it was not necessary to model or simulate any nonlinearities or indeed any other components beyond the static I-V relationship of the diodes. The interdependencies of multiple nonlinear components already show the challenges of fully modelling even the core clipping stage of the DS-1 [35].

The results at 1kHz show a divergence between real and simulated diodes. This appears to result from a combination of the low-pass filtering in the DSP code (needed for stability) and the phase shift between voltage and current induced by the digital processing latency. The necessity of this filtering shows that our approach is not immune from the stability issues of fast explicit methods that are also seen in full digital modelling of analog circuits [2]. Our synthetic approach also shows a higher noise floor compared to the real diodes, perhaps due to the limited bit depth of the DAC and noise in the level shifting circuits. Extensions to our proof of concept could easily improve these factors, achieving higher sample rates, low latencies and lower noise floors.

Other limitations of the current implementation include: a high sensitivity to miscalibration, particularly if the synthetic element is DC-coupled to the circuit; a limited range of output current imposed by the voltage swing of V_{out}, the resistance $\mathrm{R_{out}}$ and the current drive capability of op amp U2B; and a sensitivity to high frequency oscillation if sufficient analog or digital filtering is not included. The first two issues can be addressed with improvements to the analog design, while the third can be mitigated by increasing sample rate and decreasing latency.

6.1. Applications and Extensions

This paper has demonstrated how digital signal processing can be used to implement a synthetic circuit element which integrates into a larger analog circuit, without the typical impedance boundaries and unidirectional signal flow of modular audio systems. Our case study focuses on simulating a single static nonlinearity, but the same principles can be used to simulate reactive elements such as inductors and capacitors and even entire networks of analog components, as seen in the original work on vibration damping [7, 31]. Neural networks could be incorporated for simulating nonlinearities from measured data, as they have been in WDFs [21].

Incorporating synthetic impedance elements into real circuits allows new forms of real-time control and modulation, since the impedance relationship can be altered on the fly, including in response to external sensor inputs. It is also possible to replicate V-I relationships that would be impractical with real analog circuits, such as large inductors or different forms of nonlinearity. The archetypical application for our approach is not to digitally replicate an entire existing circuit, or to remove the practical dependencies on analog hardware. Rather, the main benefit is in modifying analog circuits without full replacement, especially when those circuits contain elements that are undesirable to remove because of their signature sound (e.g. classic tube-based circuits, vintage transformers or bucket-brigade delay ICs) or because they are inherently coupled to the physical domain (e.g. pickups, microphones and loudspeakers). The hybrid analog-digital circuits enabled by impedance synthesis can open up new creative possibilities for designers of audio effects and musical instruments.

7. ACKNOWLEDGMENTS

This research was supported by a UKRI Frontier Research (Consolidator) grant EP/X023478/1 (RUDIMENTS) and by the Royal Academy of Engineering under the Research Chairs and Senior Research Fellowships scheme.

Input Freq. (Hz)	Input Level (V peak)	In or Out of DS-1	Diode Type	Tone Control	Diode Config	THD (dB)	SNR (dB)	Harmonic Levels (dB)			
								2nd	3rd	4th	5th
100	±1	Out	Real	–	1F1R	-15.0	45.7	-54.6	-15.2	-60.6	-28.8
100	±1	Out	Synthetic	–	1F1R	-18.0	35.3	-40.3	-18.1	-46.2	-36.1
100	±1	Out	Synthetic	–	2F1R	-15.7	28.6	-17.1	-21.9	-40.5	-31.5
100	±1	Out	Synthetic	–	4F1R	-14.7	31.5	-15.5	-23.5	-40.3	-28.8
100	±2	Out	Real	–	1F1R	-11.1	38.6	-68.3	-12.0	-62.1	-19.1
100	±2	Out	Synthetic	–	1F1R	-13.0	35.7	-52.2	-13.5	-47.6	-23.2
100	±2	Out	Synthetic	–	2F1R	-13.6	35.4	-15.8	-18.4	-27.4	-32.9
100	±2	Out	Synthetic	–	4F1R	-12.8	37.1	-14.7	-18.3	-24.6	-34.6
1000	±1	Out	Real	–	1F1R	-15.0	46.2	-55.8	-15.2	-61.9	-28.9
1000	±1	Out	Synthetic	–	1F1R	-38.6	20.1	-43.9	-42.7	-48.4	-63.7
1000	±1	Out	Synthetic	–	2F1R	-27.1	20.9	-33.0	-37.8	-43.1	-30.0
1000	±1	Out	Synthetic	–	4F1R	-29.6	20.1	-34.2	-42.7	-40.3	-36.5
1000	±2	Out	Real	–	1F1R	-11.1	39.3	-71.3	-12.1	-64.7	-19.2
1000	±2	Out	Synthetic	–	1F1R	-43.8	25.0	-46.9	-52.5	-57.9	-53.3
1000	±2	Out	Synthetic	–	2F1R	-30.2	35.1	-32.9	-34.7	-43.2	-48.5
1000	±2	Out	Synthetic	–	4F1R	-27.9	32.3	-30.8	-32.1	-43.7	-50.2
100	±1	In	Real	Min	1F1R	-10.3	32.0	-12.9	-17.2	-17.9	-35.8
100	±1	In	Synthetic	Min	1F1R	-15.7	39.2	-21.0	-18.8	-24.0	-32.6
100	±2	In	Real	Min	1F1R	-7.5	29.5	-9.3	-37.9	-12.9	-31.1
100	±2	In	Synthetic	Min	1F1R	-13.6	36.3	-16.2	-23.7	-19.6	-34.1
1000	±1	In	Real	Min	1F1R	-7.5	36.8	-8.02	-17.6	-45.3	-27.7
1000	±1	In	Synthetic	Min	1F1R	-12.1	20.2	-12.5	-23.0	-37.0	-45.4
1000	±2	In	Real	Min	1F1R	-0.3	25.9	-0.8	-14.2	-15.5	-24.5
1000	±2	In	Synthetic	Min	1F1R	-11.2	22.4	-11.7	-22.0	-31.3	-35.8
100	±1	In	Real	Max	1F1R	-8.7	12.6	-14.2	-19.2	-16.4	-28.7
100	±1	In	Synthetic	Max	1F1R	-8.5	24.8	-10.3	-20.4	-18.4	-22.7
100	±2	In	Real	Max	1F1R	-7.5	10.2	-13.0	-22.1	-16.1	-16.9
100	±2	In	Synthetic	Max	1F1R	-7.3	18.4	-10.0	-20.6	-16.6	-20.7
1000	±1	In	Real	Max	1F1R	1.9	12.4	-0.2	-5.8	-32.4	-10.9
1000	±1	In	Synthetic	Max	1F1R	-3.7	22.0	-4.8	-11.2	-22.5	-28.8
1000	±2	In	Real	Max	1F1R	-7.5	-0.8	-21.8	-9.6	-27.9	-14.3
1000	±2	In	Synthetic	Max	1F1R	-0.6	19.8	-1.3	-13.8	-14.0	-19.8
100	±1	In	Synthetic	Min	2F1R	-9.0	43.2	-9.8	-20.3	-21.5	-29.0
100	±1	In	Synthetic	Min	4F1R	-9.5	45.6	-10.3	-20.8	-21.5	-29.3
100	±2	In	Synthetic	Min	2F1R	-8.5	38.2	-9.2	-20.9	-19.9	-27.1
100	±2	In	Synthetic	Min	4F1R	-8.9	36.1	-9.8	-21.5	-20.0	-27.3
100	±1	In	Synthetic	Max	2F1R	-8.5	25.2	-10.3	-20.8	-18.1	-22.7
100	±1	In	Synthetic	Max	4F1R	-8.9	24.3	-11.0	-20.6	-18.4	-22.8
100	±2	In	Synthetic	Max	2F1R	-7.4	18.4	-10.0	-20.7	-16.7	-20.8
100	±2	In	Synthetic	Max	4F1R	-7.8	18.3	-10.6	-20.9	-16.7	-21.4

Table 1: *Total Harmonic Distortion (THD), Signal to Noise Ratio (SNR), and individual harmonic levels relative to the fundamental for the real 1N4148 and the synthetic diode pair in isolation (out of circuit) and in different configurations in the circuit within the Boss DS-1 pedal.*

8. REFERENCES

[1] Vesa Välimäki, Federico Fontana, Julius O Smith, and Udo Zolzer, "Introduction to the special issue on virtual analog audio effects and musical instruments," *IEEE Transactions on Audio, Speech, and Language Processing*, vol. 18, no. 4, pp. 713–714, 2010.

[2] Michele Ducceschi and Stefan Bilbao, "Non-iterative simulation methods for virtual analog modelling," *IEEE/ACM Transactions on Audio, Speech, and Language Processing*, vol. 30, pp. 3189–3198, 2022.

[3] Stefan Bilbao, Charlotte Desvages, Michele Ducceschi, Brian Hamilton, Reginald Harrison-Harsley, Alberto Torin, and Craig Webb, "Physical Modeling, Algorithms, and Sound Synthesis: The NESS Project," *Computer Music Journal*, vol. 43, no. 2-3, pp. 15–30, June 2019.

[4] David Wessel and Matthew Wright, "Problems and Prospects for Intimate Musical Control of Computers," *Computer Music Journal*, vol. 26, no. 3, pp. 11–22, 2002.

[5] Matthew Davison, Andrew McPherson, Craig Webb, and Michele Ducceschi, "A Self-Sensing Haptic Actuator for Tactile Interaction with Physical Modelling Synthesis," Oct. 2024, Proceedings of the International Conference on New Interfaces for Musical Expression.

[6] Andrew McPherson, Landon Morrison, Matthew Davison, and Marcelo M. Wanderley, "On mapping as a technoscientific practice in digital musical instruments," *Journal of New Music Research*, pp. 1–16, Jan. 2025.

[7] Andrew J. Fleming, Sam Behrens, and S. O. Reza Moheimani, "Innovations in piezoelectric shunt damping," in *Smart Structures and Devices*, 2001, vol. 4235, pp. 89 – 101.

[8] Garnet Hertz and Jussi Parikka, "Zombie media: Circuit bending media archaeology into an art method," *Leonardo*, vol. 45, no. 5, pp. 424–430, 2012.

[9] Ezra J. Teboul, Andreas Kitzmann, and Einar Engström, *Modular Synthesis: Patching Machines and People*, Focal Press, London, 1st edition, Apr. 2024.

[10] Andre Almeida, David George, John Smith, and Joe Wolfe, "The clarinet: How blowing pressure, lip force, lip position and reed "hardness" affect pitch, sound level, and spectrum," *The Journal of the Acoustical Society of America*, vol. 134, no. 3, pp. 2247–2255, 2013.

[11] Arthur Paté, Jean-Loïc Le Carrou, and Benoît Fabre, "Predicting the decay time of solid body electric guitar tones," *The Journal of the Acoustical Society of America*, vol. 135, no. 5, pp. 3045–3055, 2014.

[12] Jussi Pekonen and Vesa Välimäki, "The brief history of virtual analog synthesis," in *Proc. 6th Forum Acusticum. Aalborg, Denmark: European Acoustics Association*, 2011, pp. 461–466.

[13] Charles Batchelor, Jack Gooding, William Marriott, Nikola Chalashkanov, Nick Tucker, and Rebecca Margetts, "Guitar pickups I: Analysis of the effect of winding and wire gauge on single coil electric guitar pickups," *arXiv preprint arXiv:2409.19782*, 2024.

[14] Alice Eldridge, Chris Kiefer, Dan Overholt, and Halldor Ulfarsson, "Self-resonating vibrotactile feedback instruments ||: Making, playing, conceptualising :||," in *Proc. New Interfaces for Musical Expression*, 2021.

[15] Tom Mudd, "Playing with feedback: Unpredictability, immediacy, and entangled agency in the no-input mixing desk," in *Proceedings of the 2023 CHI Conference on Human Factors in Computing Systems*, 2023, pp. 1–11.

[16] Peter Blasser, *Stores at the Mall*, Master of Arts, Wesleyan University, Middletown, CT, 2015.

[17] David T Yeh, Jonathan S Abel, and Julius O Smith, "Simplified, physically-informed models of distortion and overdrive guitar effects pedals," in *Proc. of the 10th Int. Conference on Digital Audio Effects (DAFx-07)*, Bordeaux, France, 2007.

[18] A. Fettweis, "Wave digital filters: Theory and practice," *Proceedings of the IEEE*, vol. 74, no. 2, pp. 270–327, 1986.

[19] Giovanni De Sanctis and Augusto Sarti, "Virtual analog modeling in the wave-digital domain," *IEEE transactions on audio, speech, and language processing*, vol. 18, no. 4, pp. 715–727, 2009.

[20] Kurt James Werner, Vaibhav Nangia, Julius O Smith III, and Jonathan S Abel, "Resolving wave digital filters with multiple/multiport nonlinearities," in *Proc. 18th Conf. Digital Audio Effects*, 2015, pp. 387–394.

[21] Riccardo Giampiccolo, Sebastian Cristian Gafencu, and Alberto Bernardini, "Explicit modeling of audio circuits with multiple nonlinearities for virtual analog applications," *IEEE Open Journal of Signal Processing*, 2025.

[22] Rafael C. D. Paiva, Stefano D'Angelo, Jyri Pakarinen, and Vesa Välimäki, "Emulation of Operational Amplifiers and Diodes in Audio Distortion Circuits," *IEEE Transactions on Circuits and Systems II*, vol. 59, no. 10, pp. 688–692, 2012.

[23] Stefano D'Angelo, Leonardo Gabrielli, and Luca Turchet, "Fast Approximation of the Lambert W Function for Virtual Analog Modelling," *Proceedings of the 22nd International Conference on Digital Audio Effects (DAFx-19)*, 2019.

[24] Romain Boulandet, *Tunable Electroacoustic Resonators through Active Impedance Control of Loudspeakers*, PhD thesis, EPFL, 2012.

[25] Kaijun Yi, Gaël Matten, Morvan Ouisse, Emeline Sadoulet-Reboul, Manuel Collet, and Gaël Chevallier, "Programmable metamaterials with digital synthetic impedance circuits for vibration control," *Smart Materials and Structures*, vol. 29, no. 3, pp. 035005, Mar. 2020.

[26] Foster, "A Reactance Theorem," *Bell System Technical Journal*, vol. 3, no. 2, pp. 259–267, 1924.

[27] Otto Brune, *Synthesis of a Finite Two-Terminal Network Whose Driving-Point Impedance is a Prescribed Function of Frequency*, Ph.D. thesis, Massachusetts Institute of Technology, Dept. of Electrical Engineering, 1931.

[28] Arnold E. Nordeng, "Impedance synthesizer," U.S. Patent US656542A2, 1995, Assignee: Fluke Corporation.

[29] Zdeněk Plíva, Milan Kolář, Petr Došek, and Tomáš Sluka, "A Piezoelectric Elements and Their Electronics Driving with Help of FPGA Circuits," *Ferroelectrics*, vol. 351, no. 1, pp. 187–195, June 2007.

[30] Gaël Matten, Manuel Collet, Scott Cogan, and Emeline Sadoulet-Reboul, "Synthetic Impedance for Adaptive Piezoelectric Metacomposite," *Procedia Technology*, vol. 15, pp. 84–89, 2014.

[31] J. Nečásek, J. Václavík, and P. Marton, "Digital synthetic impedance for application in vibration damping," *Review of Scientific Instruments*, vol. 87, no. 2, pp. 024704, Feb. 2016.

[32] G Raze, A Jadoul, S Guichaux, V Broun, and G Kerschen, "A digital nonlinear piezoelectric tuned vibration absorber," *Smart Materials and Structures*, vol. 29, no. 1, pp. 015007, 2019.

[33] Obaidullah Alfahmi, Christopher Sugino, and Alper Erturk, "Duffing-type digitally programmable nonlinear synthetic inductance for piezoelectric structures," *Smart Materials and Structures*, vol. 31, no. 9, pp. 095044, Sept. 2022.

[34] Brett Miller and Muhammad Iqbal, "Build your own DS-1 distortion," Online, 2010, Available at: `https://www.freestompboxes.org/members/5thumbs/BuildYourOwnDS-1Distortion.pdf`. Accessed on 2025-03-24.

[35] David T Yeh, Jonathan Abel, and Julius O Smith, "Simulation of the diode limiter in guitar distortion circuits by numerical solution of ordinary differential equations," in *Proceedings of the 10th International Conference on Digital Audio Effects (DAFx-07)*, 2007.

[36] W. Shockley, "The theory of p-n junctions in semiconductors and p-n junction transistors," *The Bell System Technical Journal*, vol. 28, no. 3, pp. 435–489, July 1949.